Dispersion Analysis for a TLM Mesh of Symmetrical Condensed Nodes with Stubs

Juan A. Morente, Gonzalo Giménez, Jorge A. Portí, and Mohsine Khalladi

Abstract— **In this paper, the dispersion characteristics of a TLM mesh formed by interconnected symmetrical condensed nodes with stubs are calculated using two different formulations. The dispersion relation derived is an implicit function of the wave number, frequency, dielectric permittivity, and magnetic permeability. Group and phase velocities are obtained for the three fundamental directions and different values of the relative permittivity. The study demonstrates that an increase in the modeled-medium permittivity leads to a decrease in the cutoff frequency for TLM numerical results.**

I. Introduction

THE Transmission-Line Modelling (TLM) method is a conceptual model that produces a time-domain numerical technique for solving fields and networks. As with any numerical method based on a segmentation of space and time, TLM implies undesired dispersion to be present in the numerical results. Several authors have studied the dispersion problem in a TLM mesh of symmetrical-condensed nodes without stubs [1]–[4], proving that it has characteristics similar to those of the finite-differences time-domain method [4]. P. B. Johns developed with the condensed node with stubs [5] a TLM structure in which extra inductances and capacitances are locally added to the node, so allowing the structure to be used for modelling anisotropic and inhomogeneous media. In this paper, two different formulations for obtaining the dispersion relation of the TLM mesh of symmetrical condensed nodes with stubs are presented, both formulations providing identical numerical results that serve as numerical validation of the proposed expressions. The numerical analysis of these dispersion relations allows the phase and group velocities to be obtained as a function of the frequency for the three fundamental directions in a TLM mesh and also for different values of the dielectric permittivity ϵ_r.

II. Derivation of the Dispersion Relation

To obtain the dispersion relation in a TLM mesh of symmetrical condensed nodes with stubs, it is advisable to undertake a similar analysis to that of the stubless node [1], [2]. Let us therefore consider the two nodes shown in Fig. 1: node C is a conventional symmetrical condensed node, and node D, whose 12 principal lines are the 12 principal transmission lines belonging to the six nodes adjacent to C. Two different formulations to obtain the dispersion relation are proposed in this paper. The first is based on the separation of voltages at node C in the stubs and the 12 principal lines contribution. The second formulation, however, considers C to be a symmetrical condensed node with stubs and D to be formed with the 12 transmission lines belonging to the six nodes adjacent to C plus the stub ports of node C. Thus, while the first method involves the use of 12×12 matrices, 18x18 matrices are required for the second.

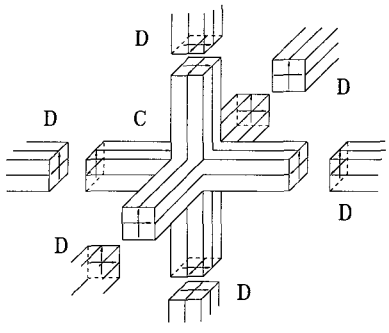

Fig. 1. Nodes C and D used to calculate the dispersion relation.

A. Formulation with 12 × 12 Matrices

Let us consider a symmetrical condensed node with stubs and divide the scattering matrix, with dimensions of 18x18, into four sub-matrices, S(12x12), G(12x6), E(6x12), H(6x6):

$$S_{\text{stub}} = \begin{bmatrix} S & G \\ E & H \end{bmatrix}. \tag{1}$$

This matrix allows us to relate the 18 incident and reflected voltages at node C and time $t_n = n\Delta t + t_0$, represented by vectors $[V_c^i]_{t_n}$ and $[V_c^r]_{t_n}$, by the equation [5]:

$$[V_c^r]_{t_n} = S_{stub}[V_c^i]_{t_n}. \tag{2}$$

However, because the propagation is only carried out through the 12 principal transmission lines that connect nodes C and D, it is advisable to divide vectors $[V_c^i]_{t_n}$ and $[V_c^r]_{t_n}$ into two contributions. One is related to the 12 principal lines, represented by the vectors $[v_c^i]_{t_n}$ and $[v_c^r]_{t_n}$ with 12 elements, and the other involves the stub voltages, denoted by vectors $[v_{c,s}^i]_{t_n}$ and $[v_{c,s}^r]_{t_n}$ with six elements each. Therefore, the incident and reflected voltages can be expressed by

$$[V_c^r]_{t_n} = \begin{bmatrix} v_c^r \\ v_{c,s}^r \end{bmatrix}_{t_n}; \quad [V_c^i]_{t_n} = \begin{bmatrix} v_c^i \\ v_{c,s}^i \end{bmatrix}_{t_n}, \tag{3}$$

Manuscript received December 23, 1993; revised March 29, 1994. This work was supported in part by "Comisión Interministerial de Ciencia y Tecnología (CICYT)" of Spain under project number TIC92-0663.

The authors are with the Departamento de Física Aplicada, Facultad de Ciencias, Universidad de Granada, 18071 Granada Spain.

IEEE, Log Number 9407305.

and, at a generic time $t_n = n\Delta t + t_0$, the voltages reflected at the 12 lines and stubs are

$$\begin{aligned}[\mathrm{v_c^r}]_{t_n} &= \mathrm{S}[\mathrm{v_c^i}]_{t_n} + \mathrm{G}[\mathrm{v_{c,s}^i}]_{t_n},\\ [\mathrm{v_{c,s}^r}]_{t_n} &= \mathrm{E}[\mathrm{v_c^i}]_{t_n} + \mathrm{H}[\mathrm{v_{c,s}^i}]_{t_n},\end{aligned} \tag{4}$$

respectively.

Unlike the node without stubs, this node stores energy in the stubs as time goes by. This fact demands the use of a numerical-process time analysis in order to obtain the relations between the incident and reflected voltages at the node at a particular moment.

Let us consider an initial time t_0, for which there is no energy in the stubs, that is to say, $[v_{c,s}^i]_{t_o} = 0$. Thus, by using (4), we may easily obtain

$$\begin{aligned}[\mathrm{v_c^r}]_{t_0} &= \mathrm{S}[\mathrm{v_c^i}]_{t_0},\\ [\mathrm{v_{c,s}^r}]_{t_0} &= \mathrm{E}[\mathrm{v_c^i}]_{t_0}.\end{aligned} \tag{5}$$

At a later time $t_1 = \Delta t + t_0$, the voltages incident at the node through the three open and three closed stubs are related with the reflected voltages at time t_0 by

$$[v_{c,s}^i]_{t_1} = Q[v_{c,s}^r]_{t_0}\ , \tag{6}$$

Q being a diagonal matrix with $\mathrm{Q}_{ii} = 1$ for i =1, 2, and 3 (open stubs) and $Q_{ii} = -1$ for i =4, 5, and 6 (short-circuited stubs). Thus, by combining (4)–(6), it may be seen that

$$\begin{aligned}[\mathrm{v_c^r}]_{t_1} &= \mathrm{S}[\mathrm{v_c^i}]_{t_1} + \mathrm{GQE}[\mathrm{v_c^i}]_{t_0},\\ [\mathrm{v_{c,s}^r}]_{t_1} &= \mathrm{E}[\mathrm{v_c^i}]_{t_1} + \mathrm{HQE}[\mathrm{v_c^i}]_{t_0}.\end{aligned} \tag{7}$$

At time $t_2 = 2\Delta t + t_0$ and keeping in mind that

$$[v_{c,s}^i]_{t_2} = Q[v_{c,s}^r]_{t_1}\ , \tag{8}$$

it is verified that

$$[\mathrm{v_c^r}]_{t_2} = \mathrm{S}[\mathrm{v_c^i}]_{t_2} + \mathrm{GQ}\left[\mathrm{E}[\mathrm{v_c^i}]_{t_1} + \mathrm{HQE}[\mathrm{v_c^i}]_{t_0}\right] \tag{9}$$

and

$$[\mathrm{v_{c,s}^r}]_{t_2} = \mathrm{E}[\mathrm{v_c^i}]_{t_2} + \mathrm{HQ}\left[\mathrm{E}[\mathrm{v_c^i}]_{t_1} + \mathrm{HQE}[\mathrm{v_c^i}]_{t_0}\right]. \tag{10}$$

Carrying out this iterative procedure until a generic time $t_n = n\Delta t + t_0$, the voltages reflected at the lines of node C are found to be (11) and (12), shown at the bottom of the page. However, because the propagation is carried out through the 12 principal lines, we will only use for our purpose (11), which provides the voltage vector reflected to these lines.

Let us now suppose that a plane wave of frequency ω is propagating through the TLM symmetrical-condensed node mesh. The incident voltages at time t_n and t_{n-1} will be related by

$$\mathrm{V_c^i}(\mathrm{t_n} - \Delta\mathrm{t}) = \mathrm{e}^{-\mathrm{j}\omega\Delta\mathrm{t}}\mathrm{V_c^i}(\mathrm{t_n}). \tag{13}$$

Since the time delay or numerical time-step, Δt, is connected with the lattice constant, Δl, by means of the relationship Δl=$\Delta t/2c$, the propagation constant of the wave in the vacuum, k_o, is related with the frequency ω through $\omega\Delta t = k_o\Delta$l/2. So, the time-delays appearing in (13) can be eliminated by using a 12x12 diagonal transmission matrix, denoted by T, whose non-zero elements are $T_{ii} = e^{-jKo\Delta l/2}$ for i =1,...,12. By doing so, we obtain that

$$[\mathrm{v_c^r}]_{t_n} = [\mathrm{S} + \mathrm{GQ}\left[\mathrm{ET} + \mathrm{HQET}^2 + \mathrm{HQHQET}^3 + \cdots\right]][\mathrm{v_c^i}]_{t_n}, \tag{14}$$

which, due to the fact that matrices T, H,and Q are diagonal, gives us

$$[\mathrm{v_c^r}]_{t_n} = [\mathrm{S} + \mathrm{GQT_sAE}][\mathrm{v_c^i}]_{t_n}, \tag{15}$$

where $T_s = e^{-jKo\Delta l/2}\mathrm{I}_o$, I_o being the 6x6 identity matrix, and A a 6x6 matrix given by the following summation:

$$\mathrm{A} = \sum_{\mathrm{n}=0}^{\infty}[\mathrm{HQT_s}]^{\mathrm{n}}. \tag{16}$$

Let us note that the upper limit of the summation for A has been supposed to be infinite because the stubs are continuously storing and giving back energy.

In addition to (15), the incident and reflected voltages at both nodes C and D ($[\mathrm{v_c^i}]_{t_n}$,$[\mathrm{v_d^i}]_{t_n}$, $[\mathrm{v_c^r}]_{t_n}$, $[\mathrm{v_d^r}]_{t_n}$) are related by the following conditions [1]:

- Propagation between adjacent nodes condition

$$[v_c^i]_{t_n} = T[v_d^r]_{t_n}\ . \tag{17}$$

- Floquet's theorem, i.e., monochromatic wave condition

$$[v_d^r]_{t_n} = P[v_c^r]_{t_n}\ . \tag{18}$$

where T is the above-defined diagonal transmission matrix that connects nodes D and C, and can be expressed by $T = e^{-jKo\Delta l/2}I$ (I is a 12x12 unit matrix), and P is a nondiagonal 12x12 matrix whose nonzero elements are

$$\begin{aligned}&\mathrm{P}_{1,12} = P_{5,7} = e^{jKy\Delta l}, \quad \mathrm{P}_{2,9} = P_{4,8} = e^{jKz\Delta l},\\ &\mathrm{P}_{3,11} = P_{6,10} = e^{jKx\Delta l}, \quad \mathrm{P}_{7,5} = P_{12,1} = e^{-jKy\Delta l}\\ &\mathrm{P}_{8,4} = P_{9,2} = e^{-jKz\Delta l}, \quad \mathrm{P}_{10,6} = P_{11,3} = e^{-jKx\Delta l}\end{aligned} \tag{19}$$

k_x, k_y, and k_z being the components of the plane-wave propagation constant in the TLM mesh.

Combining (15), (17), and (18), the following dispersion relation can be obtained:

$$\det[\mathrm{I} - \mathrm{TPS} - \mathrm{TPGQT_sAE}] = 0, \tag{20}$$

which is an implicit function of the frequency and wave number.

$$[\mathrm{v_c^r}]_{t_n} = \mathrm{S}[\mathrm{v_c^i}]_{t_n} + \mathrm{GQ}\left[\mathrm{E}[\mathrm{v_c^i}]_{t_{n-1}} + \mathrm{HQE}[\mathrm{v_c^i}]_{t_{n-2}} + \mathrm{HQHQE}[\mathrm{v_c^i}]_{t_{n-3}} + \cdots\right] \tag{11}$$

$$[\mathrm{v_{c,s}^r}]_{t_n} = \mathrm{E}[\mathrm{v_c^i}]_{t_n} + \mathrm{HQ}\left[\mathrm{E}[\mathrm{v_c^i}]_{t_{n-1}} + \mathrm{HQE}[\mathrm{v_c^i}]_{t_{n-2}} + \mathrm{HQHQE}[\mathrm{v_c^i}]_{t_{n-3}} + \cdots\right]. \tag{12}$$

B. Formulation with 18 × 18 Matrices

Let us consider two nodes, C and D, as before, but now C is a symmetrical condensed node with stubs, and D is formed by all the transmission lines that can be reached at time $t+\Delta t$ by pulses reflected at node C and previous time t. Node D is then formed by 12 transmission lines belonging to the six nodes adjacent to node C and the six stub ports belonging to node C.

The first relationship between reflected and incident voltages at node C is given by the 18x18 scattering matrix S_{stub} of the symmetrical condensed node with stubs,

$$[V_c^r]_{t_n} = S_{stub}[V_c^i]_{t_n} . \tag{21}$$

The time delay of the wave propagating from node D to node C can be summarized in matrix form as

$$[V_c^i]_{t_n} = T_{stub}[V_d^r]_{t_n} . \tag{22}$$

where $T_{\boldsymbol{stub}}$ is a diagonal 18x18 matrix whose nonzero elements are $T_{\boldsymbol{stub}\ ii} = e^{-jKo\Delta l/2}$, for i =1,...,15, and $T_{\boldsymbol{stub}\ ii} = -e^{-jKo\Delta l/2}$, for i =16, 17, and 18. The minus sign in the last elements of matrix $T_{\boldsymbol{stub}}$ is due to the fact that these stub ports are short circuited, so the reflection coefficient equals -1.

Floquet's theorem forces the monochromatic wave condition and can be expressed by means of a new 18x18 matrix, denoted by P_{stub}, in such a way that the following relation can be obtained

$$[V_d^r]_{t_n} = P_{stub}[V_c^r]_{t_n} . \tag{23}$$

The first 12 rows and columns in P_{stub} are equal to P in (19) and the rest of the elements are zero except the six belonging to the diagonal, whose value equals 1, that is to say $(P_{stub})_{ii}$=1 for i =13,...,18. These last six elements are 1 because the stub ports of node C are also the stub ports of node D.

Combining (21), (22), and (23), an alternative analytic dispersion relation is obtained in the form

$$\det[\mathrm{I} - \mathrm{T_{stub}P_{stub}S_{stub}}] = 0. \tag{24}$$

III. Numerical Results

The dispersion relations (20) and (24) are implicit functions of k_x, k_y, k_z, k_o, ϵ_r and μ_r. In an isotropic medium, the dielectric permittivity is related to the characteristic admittance Y_n of the open- circuit stubs normalized to the characteristic admittance Y_o of the principal lines, by the expression $Y_n = 4(\epsilon_r - 1)$, whereas the normalized impedance Z_n of the short-circuit stubs is related to the relative permeability μ_r by $Z_n = 4(\mu_r - 1)$. Once numerically solved, the dispersion relations (20) and (24) supply identical results, thus providing a numerical validation of the proposed dispersion relations. Figs. 2–7 show the phase and group velocities, normalized to the speed of light in the modeled medium, as a function of the normalized frequency $\Delta l/\lambda_o$, for the three principal directions in a TLM mesh and also for different values of ϵ_r and μ_r =1.

It can be easily seen for both directions [1,0,0] (Figs. 2 and 3) and [1,1,1] (Figs. 4 and 5) that an increase in the modeled- medium permittivity in a TLM mesh of condensed symmetrical nodes with stubs leads to a decrease of the cutoff frequency, which is frontier between the wave-propagation and the forbidden frequency zones of the mesh. Thus, the lower-frequency zone, in which the modeled medium is considered to be nondispersive, is moved towards lower frequency values. For direction [1,1,0] (see Figs. 6 and 7), the existence of a particular value of ϵ_r, ϵ_r = 2, for which the

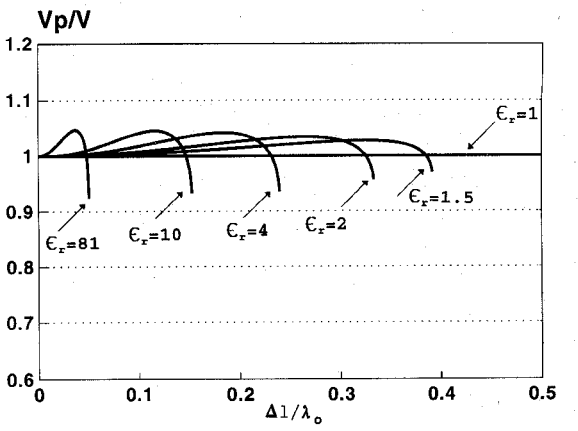

Fig. 2. Normalized phase velocity of a plane wave propagating in direction [1,0,0].

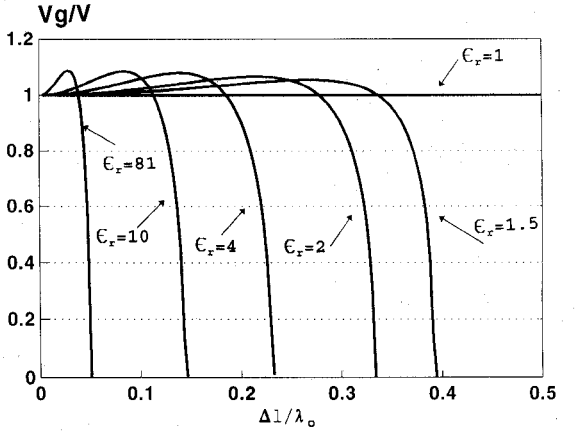

Fig. 3. Normalized group velocity of a plane wave propagating in direction [1,0,0].

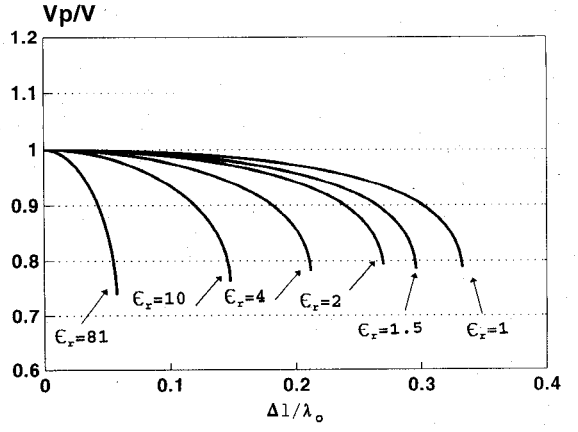

Fig. 4. Normalized phase velocity of a plane wave propagating in direction [1,1,1].

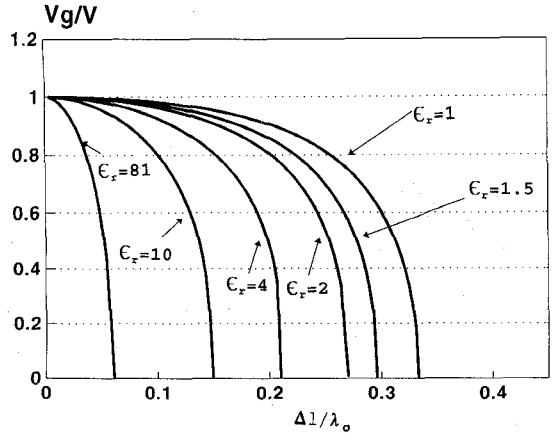

Fig. 5. Normalized group velocity of a plane wave propagating in direction [1,1,1].

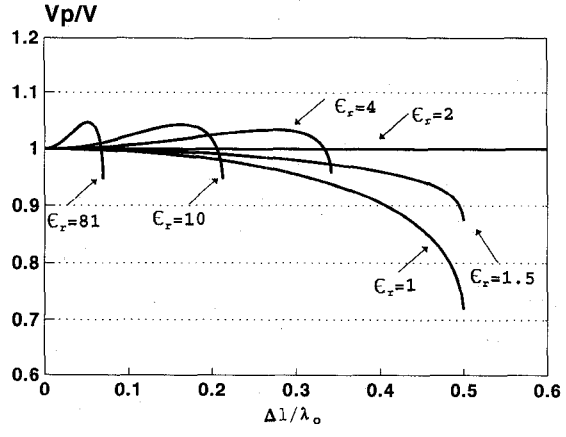

Fig. 6. Normalized phase velocity of a plane wave propagating in direction [1,1,0].

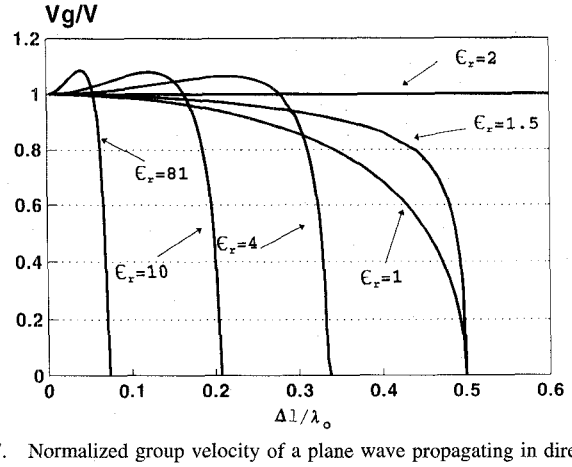

Fig. 7. Normalized group velocity of a plane wave propagating in direction [1,1,0].

TLM symmetrical-condensed-node with stubs mesh presents no dispersion, causes an improvement in the dispersive characteristics when ϵ_r is near such a value. However, an increase in ϵ_r above this particular value results in a similar behavior to that of the other directions considered.

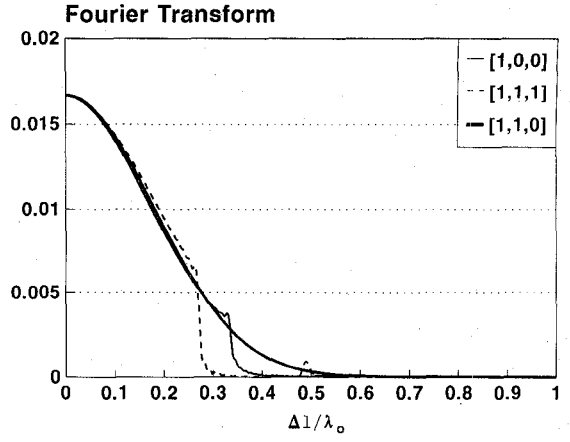

Fig. 8. Fourier transform of a plane wave with Gaussian shape after propagating through the TLM mesh with symmetrical-condensed-nodes with stubs in the three main directions for $\epsilon_r = 2$.

Let us note that the wavelength, λ, of a medium with a dielectric constant ϵ_r is related to the vacuum wavelength, λ_0, by $\lambda_0 = (\epsilon_r)^{1/2}\lambda$. For a specific frequency, this means that an increase in ϵ_r causes a decrease both in the wavelength of the modeled medium and in the bandwidth of the nondispersive region. Nevertheless, it can be observed from the results presented in Figs. 2–7 that these decreases are such that the nondispersive region in delimited by an approximate upper wavelength given by $\lambda/\Delta l = 10$, as is usual in most low-frequency numerical methods.

In order to verify the above results, we have simulated the propagation of a electromagnetic plane wave through a TLM mesh of symmetrical-condensed nodes with stubs. The mesh is a cubic domain with an edge of dimension 50Δl. The incident electric field, with a Gaussian-pulse shape and a large spectral bandwidth, is given by

$$E(t) = E_0 e^{-g^2(t-t_{max})^2}, \tag{25}$$

where $E_0 = 1$ V/m, $t_{max} = (\ln 100)^{1/2}/g, g = 0.45/\Delta t$ and $\Delta t = 1.25 \cdot 10^{-2}$ ns. The propagation along the direction [1,0,0] is simulated by exciting port 6 in each node of the $x = 3$ plane and the output is placed, in each case, at the point (10,10,10), expressed in Δl units. For direction [1,1,0], ports 5 and 6 were excited in the nodes located at plane $x + y = 6$, perpendicular to the propagation direction. Finally, propagation in the direction [1,1,1] is obtained by suitably exciting ports 2, 4, 5, and 6 of the 10 nodes contained in the $x + y + z = 6$ plane of the cubic volume modeled by the TLM lattice. Due to the absence of scatterers in the lattice, the boundary conditions were implemented by simple symmetry considerations [6].

The results are plotted in Fig. 8, which maps the Fourier transform of the electric field once it has propagated a certain distance through a medium with $\epsilon_r = 2$ along the three main directions. The appearance of the cutoffs in directions [1,0,0] and [1,1,1] can be seen, as well as the fact that they fully coincide with the values predicted by the dispersion relations previously calculated. In addition, for direction [1,1,0], the Fourier transform in the propagated field coincides with the transform of the incident field, which corroborates the

predicted absence of dispersion. It can be also noted from the direction [1,1,1] analysis that the tail of this transform rises slightly at frequency $\Delta l/\lambda_0 = 0.48$, which denotes the beginning of a spurious-mode band.

IV. Conclusion

A derivation of the dispersion relation of the TLM-symmetrical-condensed node with stubs mesh and the subsequent numerical analysis of the determinant in the dispersion relation has enabled us to obtain the phase and group velocities as a function of the frequency and dielectric permittivity for the three fundamental directions of this TLM lattice.

For directions [1,0,0] and [1,1,1], it has been shown that an increase of ϵ_r involves a reduction in the cutoff frequencies and so in the width of the desired nondispersive band. For direction [1,1,0], a TEM plane wave suffers no dispersion effects when a medium with $\epsilon_r = 2$ is numerically modeled. For higher values of the dielectric permittivity, however, this direction shows a dispersive behavior similar to that observed for the previously mentioned directions. In TLM with stubs, as with other numerical methods, the unit cell size must be of the order of 0.1 of the wavelength at the highest frequency of interest.

Acknowledgment

The authors would also like to thank Miss Christine M. Laurin for her help in preparing the manuscript.

References

[1] J. Nielsen and W. J. R. Hoefer, "A complete dispersion analysis of the condensed node TLM mesh," *IEEE Trans. Magn.*, vol. MAG-27, pp. 3982–3985, Sept. 1991.

[2] J. Nielsen, "Spurious modes for the TLM-condensed node formulation," *IEEE Microwave and Guided Wave Lett.*, vol. 1, pp. 201–203, Aug. 1991.

[3] D. H. Choi, "A comparison of the dispersion characteristics associated with the TLM and FD-TD methods,"*Int. J. Numerical Modelling: Electronic Networks, Devices and Fields,* vol. 2, pp. 203–214, 1989.

[4] J. A. Morente, G. Giménez, J. A. Portí, and M. Khalladi, "Group and phase velocities in the TLM-symmetrical-condensed-node mesh," *IEEE Trans. Microwave Theory Tech.*, vol. MTT-42, Mar. 1994.

[5] P. B. Johns, "A symmetrical condensed node for the TLM method," *IEEE Trans. Microwave Theory Tech.*, vol. MTT-35, pp. 370–377, Apr. 1987.

[6] J. A. Morente, J. A. Portí, and M. Khalladi, "Absorbing boundary conditions for the TLM method," *IEEE Trans. Microwave Theory Tech.*, vol. MTT-40, pp. 2095–2099, Nov. 1992.

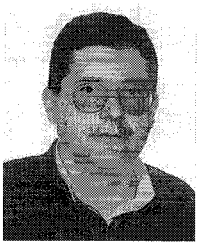

Juan A. Morente was born in Porcuna (Jaén), Spain, in 1955. He received the Licenciado and Doctor degrees in physics from the University of Granada, Spain, in 1980 and 1985, respectively.

He is presently ' "Profesor Titular"' in the Department of Applied Physics at the University of Granada. His main fields of interest include electromagnetic theory and applied mathematics. His current research activities deal with numerical analysis of physical systems and transient phenomena.

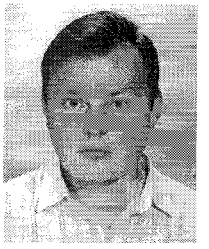

Gonzalo Giménez was born in Aguilas, (Murcia), Spain, in 1968. He received his B.Sc. degree in electronic and electrical physics in 1991 and his M.Sc. degree in Applied Physics in 1993 (University of Granada). He is currently doing his Ph.D. in the Department of Applied Physics at the University of Granada, Spain.

His current research interests deal with the numerical analysis of waveguides and transmission lines and numerical methods in applied electromagnetics

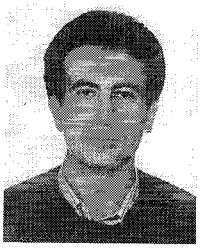

Jorge A. Portí was born in Valle de Escombreras, Cartagena, (Murcia), Spain, in 1963. He received the M.S. and Ph.D. degrees in Physics from the University of Granada, Spain, in 1988 and 1993, respectively.

From October 1988 to December 1990, he was with Fujitsu ESPAÑA, S.A. where he was engaged in data-communication switching. Since October 1990, he has been with the Department of Applied Physics at the University of Granada, Spain, where he is now assistant professor. His current research activities deal with numerical solution of transient electromagnetic problems.

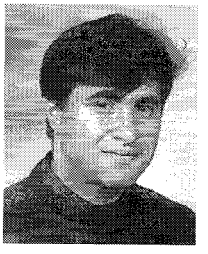

Mohsine Khalladi was born in Tangier, Morocco, on November 27, 1963. He received his B.S. degree in 1988 from the University of Abdelmalek Essaadi, Tetouan, Morocco and Ph.D. degree in physics from the University of Granada, Spain, in 1994.

Mr. Khalladi's current research interests lie in time-domain numerical solutions of scattering and electromagnetic problems.